NeuroImage: Clinical 37 (2023) 103284

Contents lists available at ScienceDirect

NeuroImage: Clinical

journal homepage: www.elsevier.com/locate/ynicl

A comparison of diffusion tensor imaging tractography and constrained spherical deconvolution with automatic segmentation in traumatic brain injury

Jussi Tallus [a,b,*], Mehrbod Mohammadian [a], Timo Kurki [a,b], Timo Roine [c,d], Jussi P. Posti [a,e], Olli Tenovuo [a]

[a] Turku Brain Injury Center, Department of Clinical Neurosciences, University of Turku and Turku University Hospital, Hämeentie 11, Turku FI-20521, Finland
[b] Department of Radiology, University of Turku and Turku University Hospital, Hämeentie 11, Turku FI-20521, Finland
[c] Turku Brain and Mind Center, University of Turku, Turku FI-20014, Finland
[d] Department of Neuroscience and Biomedical Engineering, Aalto University School of Science, Rakentajanaukio 2 C, Espoo 02150, Finland
[e] Neurocenter, Department of Neurosurgery, Turku University Hospital, University of Turku, Hämeentie 11, Turku FI-20521, Finland

ARTICLE INFO

Keywords:
Traumatic brain injury
Diffusion-weighted imaging
Tractography
Constrained spherical deconvolution
Diffusion tensor imaging

ABSTRACT

Detection of microstructural white matter injury in traumatic brain injury (TBI) requires specialised imaging methods, of which diffusion tensor imaging (DTI) has been extensively studied. Newer fibre alignment estimation methods, such as constrained spherical deconvolution (CSD), are better than DTI in resolving crossing fibres that are ubiquitous in the brain and may improve the ability to detect microstructural injuries. Furthermore, automatic tract segmentation has the potential to improve tractography reliability and accelerate workflow compared to the manual segmentation commonly used. In this study, we compared the results of deterministic DTI based tractography and manual tract segmentation with CSD based probabilistic tractography and automatic tract segmentation using TractSeg. 37 participants with a history of TBI (with Glasgow Coma Scale 13–15) and persistent symptoms, and 41 healthy controls underwent deterministic DTI-based tractography with manual tract segmentation and probabilistic CSD-based tractography with TractSeg automatic segmentation.Fractional anisotropy (FA) and mean diffusivity of corpus callosum and three bilateral association tracts were measured. FA and MD values derived from both tractography methods were generally moderately to strongly correlated. CSD with TractSeg differentiated the groups based on FA, while DTI did not. CSD and TractSeg-based tractography may be more sensitive in detecting microstructural changes associated with TBI than deterministic DTI tractography. Additionally, CSD with TractSeg was found to be applicable at lower b-value and number of diffusion-encoding gradients data than previously reported.

1. Introduction

Diffuse axonal injury (DAI) is a major contributor for morbidity in traumatic brain injury (TBI) of all severities (McGinn and Povlishock, 2016). In contrast to focal lesions that characterise more severe injuries and are visible on routine imaging, diffuse, microstructural white matter injuries may be detected in vivo only by specialised magnetic resonance imaging (MRI) methods, such as diffusion tensor imaging (DTI) (Alexander et al., 2007; Brandstack et al., 2013).

Diffusion changes typically associated with chronic TBI are decreased fractional anisotropy (FA) and increased mean diffusivity (MD), although this is not a universal pattern (Bazarian et al., 2007; Cubon et al., 2018; Mayer et al., 2010; Wilde et al., 2008). In acute to subacute TBI (roughly within 1 month), there is more variation as to whether decreased or increased FA and MD are reported (Bazarian et al., 2007; Cubon et al., 2018; Mayer et al., 2010; Wilde et al., 2008). Time-course of secondary injury development may be very long, as progressing DTI changes (Dinkel et al., 2014) and elevated levels of TBI

Abbreviations: CSD, constrained spherical deconvolution; DAI, diffuse axonal injury; DTI, diffusion tensor imaging; DWI, diffusion-weighted imaging; FA, fractional anisotropy; fODF, fibre orientation distribution function; GCS, Glasgow coma scale; GOSE, Glasgow outcome scale – extended; MD, mean diffusivity; ROI, region of interest; TBI, traumatic brain injury.

* Corresponding author at: Turku University Hospital, Hämeentie 11, Turku FI-20521, Finland.
E-mail address: jptall@utu.fi (J. Tallus).

https://doi.org/10.1016/j.nicl.2022.103284
Received 10 May 2022; Received in revised form 20 October 2022; Accepted 5 December 2022
Available online 6 December 2022

related blood biomarkers (especially neurofilament light) (Shahim et al., 2020) have been detected even years after injury in prospective studies. Depending on injury stage, possible histological mechanisms of diffusion changes include damage to myelin or axon membranes, reduced number of axons, reduced axon coherence, oedema and recruitment of compensatory mechanisms or neuroplasticity (Borja et al., 2018; Lin et al., 2016; Lipton et al., 2012; Mayer et al., 2010). Decreased FA and increased MD have been observed in many white matter tracts, with the corpus callosum being the most commonly affected structure in patients with TBI (Hulkower et al., 2013; Hunter et al., 2019). This may be due in part to selection bias though, as many studies have used predetermined regions of interest (ROIs). Abnormalities in the superior and inferior longitudinal fasciculi have been equally common in whole brain analyses, with many other structures also commonly affected (Hulkower et al., 2013).

In clinical practice, microhaemorrhages detected on T2* or susceptibility-weighted imaging sequences have been considered the most important surrogate imaging biomarker for DAI (Useche and Bermudez, 2018). MRI-detected microhaemorrhages have been associated with FA loss and MD increase in DTI (Håberg et al., 2015; Rostowsky et al., 2018). However, microhaemorrhages are a sign of diffuse vascular injury, which seems to have only modest correlation with DAI (Andreasen et al., 2020; Haber et al., 2021; Niogi et al., 2008). White matter tractography is a method for quantifying microstructural white matter integrity more directly.

The most widely used approach to tractography presently is DTI, which relies on diffusion tensors. Diffusion tensor estimates a single three-dimensional orientation for diffusion in a voxel. However, when voxels contain multiple fibre orientations, the method is less reliable (Basser et al., 2000; Basser and Pierpaoli, 1996). It has been estimated that the majority of white matter voxels contain multiple fibre orientations (Jeurissen et al., 2013). Constrained spherical deconvolution (CSD) (Jeurissen et al., 2011; Tournier et al., 2007) seeks to address the problem of multiple fibre orientations. In this approach, spherical deconvolution method is used to extract white matter fibre orientation distribution function (fODF). To date, there is evidence of CSD-based tractography correlating better than DTI with memory function in Alzheimer's disease (Reijmer et al., 2012) and motor function after stroke (Auriat et al., 2015), and depicting in more detail the relevant white matter tracts before glioma surgery (Becker et al., 2020; Mormina et al., 2016).

CSD is developed for single-shell high angular resolution diffusion imaging data (Tuch et al., 2002) with a b-value ideally at 2500–3000 s/mm^2 and 45 or more diffusion encoding gradient directions (Tournier et al., 2013), although today multi-shell based CSD estimations exist as well (Jeurissen et al., 2014; Tournier et al., 2007). However, good results have been demonstrated with CSD at b = 1000 s/mm^2 and 30 diffusion encoding gradient directions, performing superior to DTI even at such data (Calamuneri et al., 2018).

Although CSD addresses the problem of crossing fibres better than DTI, there is no unambiguous way to trace fibres through voxels with multiple fibre orientations (Maier-Hein et al., 2017). Commonly employed strategy is to apply expert anatomical knowledge to delineate tracts, by defining regions to be included or excluded (Rheault et al., 2020). The disadvantage of this method is the high amount of work and operator dependency. Automatic segmentation methods have been developed to solve these problems. In this study, we used the openly available TractSeg automatic segmentation tool (Wasserthal et al., 2018). TractSeg is based on a convolutional neural network and pretrained on high-quality diffusion MRI data acquired for the Human Connectome Project. Segmentation in TractSeg is performed on fODF peaks without prior tractography. 72 fibre bundles can be segmented and probabilistic fibre tracking is performed within these bundles to generate bundle-specific tractograms (Wasserthal et al., 2019). TractSeg is robust in eliminating false positive fibres, which would otherwise be a problem with probabilistic CSD-based tractography (Maier-Hein et al., 2017). Other semi-automated tools for tract segmentation exist, including AFQ/pyAFQ (Kruper et al., 2021; Yeatman et al., 2012), and WMA segmentation (Bullock et al., 2019).

In this study, we compared the results of deterministic DTI based tractography and manual tract segmentation with CSD based probabilistic tractography and automatic tract segmentation using TractSeg. The participant sample consisted of symptomatic patients with a history of TBI, initially defined as mild based on the GCS score, and healthy controls. CSD is superior to DTI in modelling complex fibre architectures and there are reports of its clinical superiority in non-TBI applications (see above). Therefore, we hypothesised that CSD- and TractSeg-based tractography would be superior to DTI-based tractography in detecting white matter microstructural alterations in TBI. We also examine the applicability of CSD-based analysis in combination with TractSeg in DWI data that were previously considered suboptimal or even incompatible with CSD. This may be of value, as many clinical imaging setups presently do not correspond to what is considered ideal for these applications.

2. Methods

2.1. Participants

Participants were 37 symptomatic patients with a history of TBI and 41 age and sex matched healthy controls. Patients with TBI were recruited at the TBI outpatient department of Turku University Hospital during 2013–2016. Patients were considered for inclusion if following criteria were met: a) age 18–65 years during the injury and inclusion to the study, b) no neurological comorbidities besides possible migraine, c) no psychiatric comorbidities requiring treatment (a history of mild depression or anxiety disorder was permitted, if no medication or other treatment was presently required), d) a history of non-penetrating TBI with the lowest acutely documented Glasgow coma scale (GCS) score of 13–15, d) MRI with DWI had been done according to the study protocol, e) besides possible microhaemorrhages, no evidence of trauma or other neurological disease in routine clinical MRI evaluation (e.g., no mass lesions), f) Glasgow outcome scale extended available, evaluated 6 months after injury earliest by an experienced neurologist, and scored <8, indicating incomplete recovery, g) presence of residual symptoms clinically related to TBI.

All patients had clinically obvious sequels from their TBI based on standard clinical evaluation. This was carefully assessed based on detailed history of the injury event and symptom evolution, neuropsychological evaluation, and absence of other possible causes for their symptoms. The clinical variables GCS, GOSE, post traumatic amnesia duration (PTA), and time from injury to imaging were extracted from the patient records. Controls were healthy 18–65-year-old volunteers with no history of TBI and otherwise fulfilling the same criteria. All participants gave their written informed consent. The study was accepted by the Ethical Committee of the Hospital District of Southwest Finland and carried out in accordance with The Code of Ethics of the World Medical Association (Declaration of Helsinki).

2.2. MRI acquisition

A 3.0 T MRI scanner (Achieva, Philips Medical Systems, Best, Netherlands) was used with an eight-channel sensitivity encoding transmit-receive head coil. DW imaging was performed in transverse plane with echo-planar sequence (TR 5877 ms, TE 62 ms, 60 2.0 mm slices with no gap, 112×128 reconstructed matrix, turbo factor 59, echo-planar imaging factor 59, FOV rectangular 224 mm, two signals acquired). We acquired a b = 0 s/mm^2 image and b = 800 s/mm^2 images with 15 different gradient-encoding directions. Images with isotropic 2 mm voxel size were obtained. Besides DWI, routine T1, T2, fluid-attenuated inversion recovery and susceptibility weighted imaging sequences were acquired. All images were analysed by a neuroradiologist

to ascertain that inclusion criteria were fulfilled.

2.3. DWI analysis

Images were postprocessed to remove distortions due to shear, eddy currents, and motion using Diffusion Registration Tool (Philips Medical Systems). Deterministic DTI tractography was done using the FiberTrak software (Philips Medical Systems). Analysed tracts were corpus callosum, left and right cingulum, left and right uncinate fascicle, and left and right superior longitudinal fascicle. Each was defined by two free-hand inclusion ROIs and possible one exclusion ROI. ROIs were drawn based on individual anatomy as depicted in overlaid colour coded DWI and T1 images. The ROIs were generated by JT and inspected by TK, both with a specialist degree in radiology and TK also a certified neuroradiologist. The tracts were defined in the following way: 1) The corpus callosum was defined by two inclusion ROIs drawn on sagittal images at the level of left and right cingulate gyrus, and including the corpus callosum. 2) The cingulum was defined by two inclusion ROIs drawn around the cingulum on coronal images at the level of the upper part of the aqueduct and at the level of the mammillary bodies. Also an exclusion ROI was drawn around the corpus callosum on a midline sagittal image. 3) The superior longitudinal fascicle was defined by two ROIs drawn around the fascicle on coronal images at the level of the upper part of the aqueduct and at the level of the mammillary bodies. 4) The uncinated fascicle was defined by two ROIs drawn on a single coronal image, one surrounding the most anterior part of the fascicle that could be seen traversing in anteroposterior direction in the basal frontal lobe, and the other ROI surrounding the entire anterior temporal lobe at the same level.

For tract termination a minimum FA limit 0.5 was used for corpus callosum and 0.3 for the other tracts, and a maximum angle limit of 27°. Minimum track length was set at 10 mm. These criteria were used to reconstruct each tract volume, from which average FA and MD values were calculated by the FiberTrak software.

For the CSD based tractography, DWI images were denoised (Veraart et al., 2016), corrected for Gibbs ringing artefacts (Kellner et al., 2016), eddy currents and head motion (Andersson and Sotiropoulos, 2016), and bias field (Tustison et al., 2010), comprising a similar preprocessing pipeline as in (Ades-Aron et al., 2018). MRtrix3 (Tournier et al., 2019) was used to generate fODF peaks, using the Tournier et al. (Tournier et al., 2013) iterative algorithm. Spherical harmonics up to order four were used to estimate the fODF. The fODF peaks were used as input for TractSeg to reconstruct fibre bundles, using probabilistic Tract Orientation Mapping (TOM) tractography (Wasserthal et al., 2019; Wasserthal et al., 2018).

To evaluate the effect of the more advanced preprocessing methods available in the CSD analysis pipeline, compared to the DTI pipeline, we calculated an alternative CSD and TractSeg based analysis, with only motion and eddy current correction preprocessing steps. These results are reported separately.

From both CSD + TractSeg and DTI based tractography the mean FA and MD values of selected tracts were extracted for statistical analysis. Examples of final tractograms are presented in Fig. 1.

2.4. Statistical analysis

Statistical analyses were done using IBM SPSS Statistics version 25 (IBM corp., Armonk, NY, USA) and Matlab R2021a (The MathWorks, Natick, MA, USA). Repeated measures analysis of variance (rmANOVA) was conducted, with analysis method (CSD + TractSeg or DTI) and tract (corpus callosum, and separately for each hemisphere the uncinate fascicle, cingulum, and superior longitudinal fascicle) as within-subjects variables and group (controls or TBI) as a between-subjects factor. Greenhouse-Geisser correction was applied where sphericity assumption was violated. Partial eta squared effect size estimates (η_p^2) were calculated. Independent or paired samples t-tests and Mann-Whitney U-tests with Bonferroni corrections were used for post-hoc comparisons and Chi-square test for sex distribution. Spearman rank-order correlation coefficients were calculated to evaluate the relation of clinical variables (GCS, GOSE, PTA and time from injury) to tractography statistics. Pearson's correlation coefficients were calculated to compare the FA and MD produced by each tractography method for every tract and also for a calculated mean FA and mean MD including data from all the tracts. All analyses were performed separately for the FA and MD values.

3. Results

3.1. Participant characteristics

Characteristics of the participant sample are presented in Table 1. On average, the participants with TBI had sustained the injury 1.2 years before MRI, with shortest interval being 2 weeks and longest 9.9 years. All TBIs were sustained in civilian settings, with most common mechanisms being traffic accidents and falls, and some cases of assault also included. No penetrating or blast-induced TBIs were included. All participants' TBI had been initially evaluated as mild based on GCS 13–15.

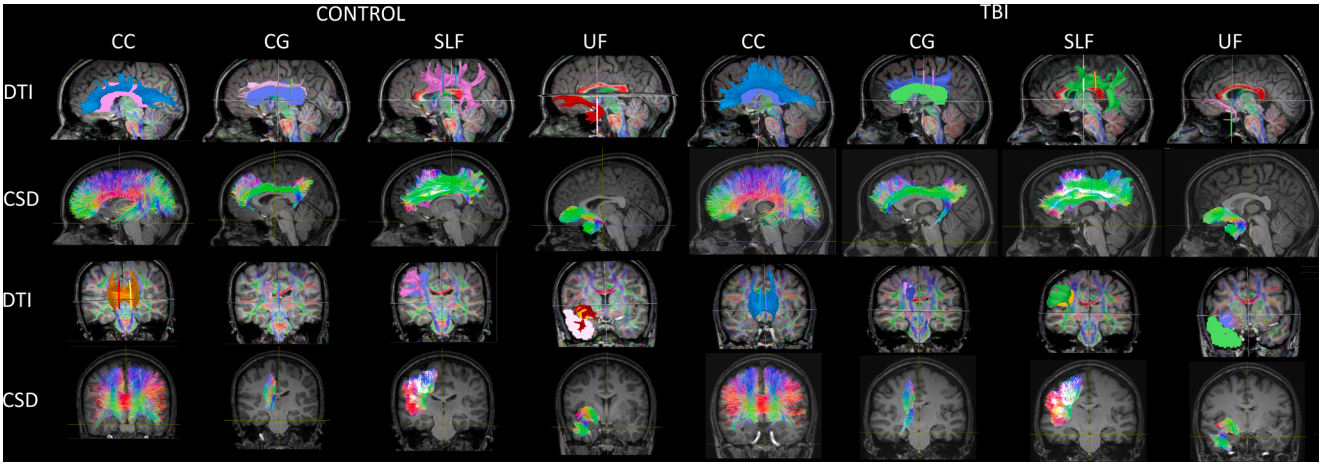

Fig. 1. Sample tractograms from DTI and CSD based tractographies. On the left a sample patient's data from the control group and on the right from the TBI group. Data from different tractography methods is organised in rows, with sagittal and coronal images shown in their own rows. Tractograms are overlaid on T1 weighted anatomical images. For DTI, the ROIs on which the tractograms are based on are also demonstrated. The left sided association tracts were defined correspondingly. CC, corpus callosum; CG, cingulum; UF, uncinated fasciculus; SLF, superior longitudinal fasciculus.

Table 1
Participant characteristics. For all variables except sex, mean ± standard deviation is reported and the minimum and maximum observed values are in parentheses. For sex and age, p-values (Chi-square test for sex and independent-samples *t*-test for age) of between groups comparisons are reported.

Group	TBI (n = 37)	Control (n = 41)	p-value
Sex	15 female 22 male	17 female 24 male	0.934
Age, years	37.2 ± 11.4 (19–60)	36.4 ± 11.9 (18–57)	0.777
GCS	14.7 ± 0.6 (13–15)		
PTA, hours	76 ± 23.0 (0–504)		
Imaging interval, years	1.2 ± 2.1 (0.04–9.9)		
GOSE	5.6 ± 1.1 (4–7)		
Microhaemorrhages	11 patients (29.7 %)		

However, 40.5 % of patients were found to have a PTA ≤ 24 h and 59.5 % had a PTA > 24 h, and 11 TBI participants (29.7 %) had micro-haemorrhages detected in clinical MRI. Depending on classification used, these features may imply a complicated mild or moderate TBI in these participants, despite initial mild level GCS. All participants had incomplete functional recovery at the time of imaging (GOSE < 8). The clinical neurological and neuropsychological evaluation results were studied from patient records and revealed common TBI related symptoms (e.g., fatigue, memory and emotional problems, minor motor symptoms).

3.2. Analysis of FA and MD values – other than group-related effects

Results of the main rmANOVAs are presented in Tables 2 and 3.

Differing FA and MD values were found for the different individual tracts, disregarding which tractography method was used (main effect of tract for FA $p < 0.001$, and MD $p < 0.001$). CSD + TractSeg based tractography resulted in generally lower FA (main effect of method $p < 0.001$) and lower MD ($p < 0.001$) values than DTI-based tractography. Participant age was found to be related to FA values (main effect of age $p < 0.001$), due to lower FA values with higher age.

An interaction was found between tractography method and tract studied ($p < 0.001$ and $\eta_p^2 = 0.615$ for FA values and $p < 0.001$ and $\eta_p^2 = 0.163$ for MD values). Based on descriptive statistics (not shown) and Fig. 2 this is due to CSD + TractSeg and DTI resulting in different relative FA and MD values for different tracts. For example, with CSD + TractSeg the highest FA values were found in the superior longitudinal fascicles, but with DTI the highest FA was found in the corpus callosum (see Fig. 2).

For FA values, we found an interaction between tract and age ($p = 0.006$, $\eta_p^2 = 0.047$). Based on analysis of scatterplots (not shown) this seems to be due to more obvious age-related declines in FA values of some tracts (e.g. the superior longitudinal fascicles), while no clear trend was seen in other tracts (e.g. the corpus callosum). This aspect of our results was not analysed further, as it was not considered essential to this study.

Table 2
Rmanova results for fa values. Main effects and interactions are reported, with F-values, Greenhouse-Geisser corrected p-values, and η_p^2 estimates of effect size. Statistically significant effects are marked with an asterisk.

	F	p	η_p^2
Sex	0.079	0.779	0.001
Age	14.152	<0.001*	0.161
Group	1.779	0.186	0.023
Tract	48.806	<0.001*	0.397
Tract × sex	2.063	0.086	0.027
Tract × age	3.660	0.006*	0.047
Tract × group	0.483	0.747	0.006
Method	818.712	<0.001*	0.917
Method × sex	2.478	0.120	0.032
Method × age	0.042	0.837	0.001
Method × group	21.027	<0.001*	0.221
Tract × method	118.206	<0.001*	0.615
Tract × method × sex	0.996	0.411	0.013
Tract × method × age	0.430	0.790	0.006
Tract × method × group	0.329	0.862	0.004

Table 3
Rmanova results for md values. Main effects and interactions are reported, with F-values, Greenhouse-Geisser corrected p-values, and η_p^2 estimates of effect size. Statistically significant effects are marked with an asterisk.

	F	p	η_p^2
Sex	0.417	0.521	0.006
Age	0.083	0.775	0.001
Group	1.580	0.213	0.021
Tract	25.394	<0.001 *	0.255
Tract × sex	3.854	0.007 *	0.050
Tract × age	1.325	0.264	0.018
Tract × group	1.328	0.263	0.018
Method	0.867	0.355	0.012
Method × sex	0.070	0.793	0.001
Method × age	0.056	0.813	0.001
Method × group	7.505	0.008 *	0.092
Tract × method	14.402	<0.001 *	0.163
Tract × method × sex	2.936	0.019 *	0.038
Tract × method × age	2.436	0.044 *	0.032
Tract × method × group	0.763	0.557	0.010

For MD values, we found also interactions of tract × sex ($p = 0.007$), tract × method × sex ($p = 0.019$), and tract × method × age ($p = 0.044$). Follow-up ANOVAs were calculated separately for each tract. It was found that MD values in corpus callosum were higher in males ($p = 0.027$). CSD + TractSeg produced lower MD values for females compared to males on right cingulate gyrus (interaction $p = 0.014$), while no sex differences were found with DTI or with either method on the left cingulate gyrus. No significant effects were found for the uncinated fascicles or the superior longitudinal fascicles. This data is not presented in more detail.

3.3. Analysis of FA and MD values – group-related effects

There was an interaction between the participant group (TBI or control) and tractography method (CSD + TractSeg or DTI) on FA values ($p < 0.001$, $\eta_p^2 = 0.221$) and with a smaller effect size on MD values ($p = 0.008$, $\eta_p^2 = 0.092$). To explain this, separate rmANOVAs were calculated for each tractography method. CSD + TractSeg resulted in lower FA values ($p = 0.008$, $\eta_p^2 = 0.091$) in the TBI group compared to the control group, while FA values derived from DTI did not differ statistically significantly between the groups ($p = 0.580$, $\eta_p^2 = 0.004$). Thus, CSD + TractSeg was able to differentiate the patient group from controls based on FA, but the same was not found for DTI.

For the MD values, follow-up rmANOVA did not reveal statistically significant effect of group on either the CSD + TractSeg-derived values ($p = 0.064$, $\eta_p^2 = 0.046$) or DTI values ($p = 0.527$, $\eta_p^2 = 0.005$). Thus, the weaker group × method interaction for MD values is not conclusively explained. Based on descriptives it may, however be related to higher MD values in TBI group compared to controls in CSD + TractSeg tractography.

Correlation analyses did not reveal correlations between the recorded background variables (GCS, GOSE, PTA and time interval from injury to imaging) and tractography results. Separate rmANOVAs were conducted to analyse the effect of time from injury to imaging to FA and MD values. In this, only TBI participants were included and time interval from injury to imaging was dichotomised, using a cutoff of 3 months to yield groups of N = 17 and N = 20. This dichotomy was used as a grouping variable and otherwise identical rmANOVAs to the ones reported above were done. No statistically significant main effects or interactions including the dichotomised time from injury to imaging were found.

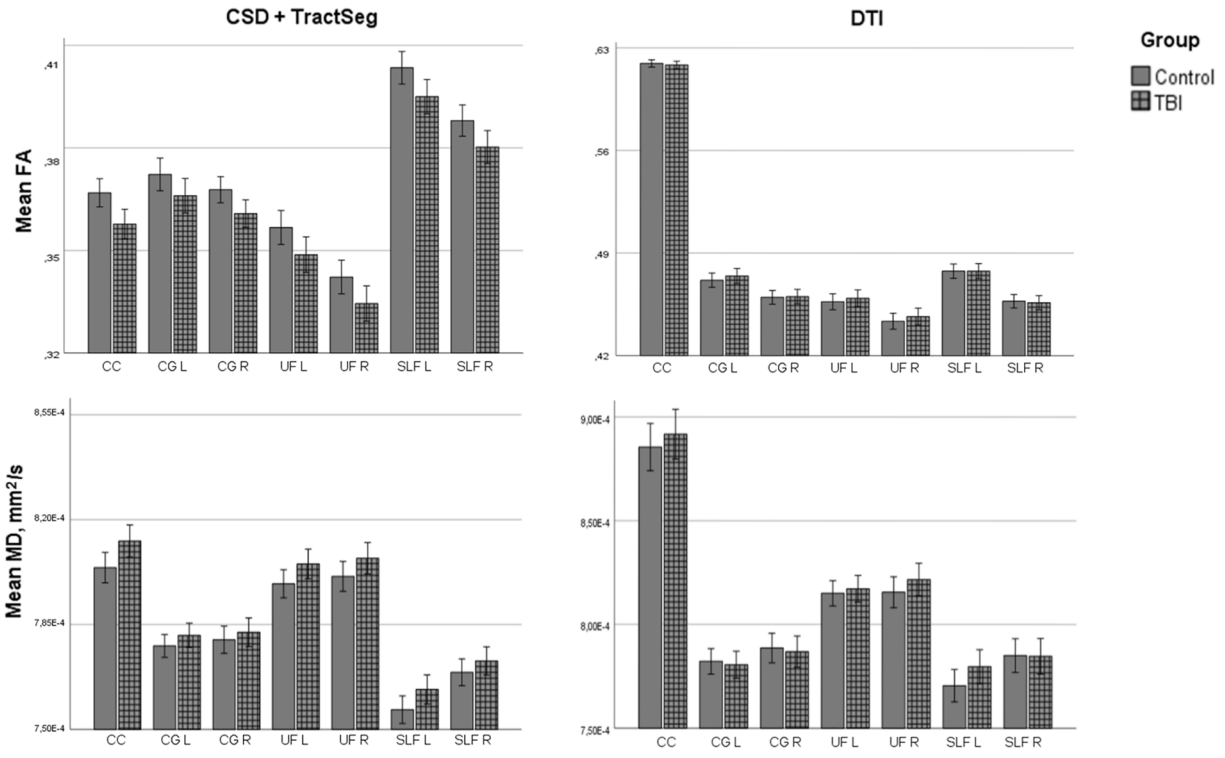

Fig. 2. Mean values ± 95 % confidence intervals of mean for each tract, separately for each group. Upper row, FA values; lower row, MD values. Left column, CSD + TractSeg; right column, DTI. CC, corpus callosum; CG, cingulum; UF, uncinated fasciculus; SLF, superior longitudinal fasciculus; L, left; R, right.

3.4. Correlation between methods

Correlation coefficients were calculated for each tract's CSD + TractSeg and DTI derived values. The results of the different tractography methods were positively correlated for every tract. Strong correlations were generally found for MD values. Most FA values were moderately or strongly correlated between the methods, with the strongest correlations found for superior longitudinal fasciculi, and only a weak (but statistically significant) correlation for the left uncinate fascicle (Table 4).

As the correlation properties of each tract were very similar, mean FA and MD values across all tracts were also calculated by adding all individual tract results and dividing by the number of tracts. This was done to allow simpler presentation of the distribution of FA and MD values and correlation of the values between DTI and CSD + TractSeg. The distributions of these compound mean FA and mean MD values separately for each tractography method and group are displayed in Fig. 3. It is noteworthy that the distributions overlap in large part, but in CSD + TractSeg derived FA values, there is a longer tail of small FA values, representing a minority of TBI patients with more deviant values.

The mean FA values measured by DTI and CSD + TractSeg were moderately strongly correlated ($r = 0.710$, $p < 0.001$). The mean MD values measured by DTI and CSD + TractSeg were strongly correlated ($r = 0.911$, $p < 0.001$). Fig. 4 visualises these correlations as scatterplots, also showing the participant groups separately.

Table 4
Pearson correlations of the different tractography methods for each tract. Correlations of both FA and MD values are indicated. CC, corpus callosum; CG, cingulum; UF, uncinated fasciculus; SLF, superior longitudinal fasciculus; L, left; R, right. Pearson correlation coefficients and p-values are reported.

	CC	CG L	CG R	UF L	UF R	SLF L	SLF R
FA	0.588	0.532	0.547	0.387	0.546	0.686	0.784
	p < 0.001	p < 0.001	p < 0.001	p < 0.001	p < 0.001	p < 0.001	p < 0.001
MD	0.825	0.828	0.855	0.762	0.832	0.876	0.852
	p < 0.001	p < 0.001	p < 0.001	p < 0.001	p < 0.001	p < 0.001	p < 0.001

3.5. Analysis with alternative preprocessing methods

To test for effect of more limited preprocessing, CSD + TractSeg tractography was done with only motion and eddy current correction. Using this data we repeated the rmANOVAs described above in sections 3.2 and 3.3. Similar results were obtained. For FA values, same statistically significant main effects and interactions were found as before (cf. Table 2), with the exceptions that the previously found tract × age interaction lost its significance, but a new interaction of method × age ($p < 0.001$) was detected.

For MD values (cf. Table 3), the interaction method × group was lost, as was the interaction tract × method × age. New statistically significant interaction method × age ($p = 0.027$) was found.

4. Discussion

The aim of this study was to compare a deterministic DTI based tractography and manual segmentation method with a CSD based probabilistic tractography and automatic tract segmentation using TractSeg. Our sample consisted of healthy controls and persistently symptomatic patients with a history of TBI and acutely evaluated GCS of 13–15. Our main finding is that CSD and automated TractSeg based tractography were able to differentiate the TBI group from a group of healthy controls, while DTI based tractography was not. This suggests that CSD and TractSeg is more sensitive at detecting microstructural injuries associated with TBI than DTI based analysis. If this is the case, CSD and TractSeg may lead to detection of clinically significant alterations in patients for whom more traditional tractography might appear normal.

The groups differed mainly on the basis of FA measured from the corpus callosum and three bilateral association tracts. The TBI group

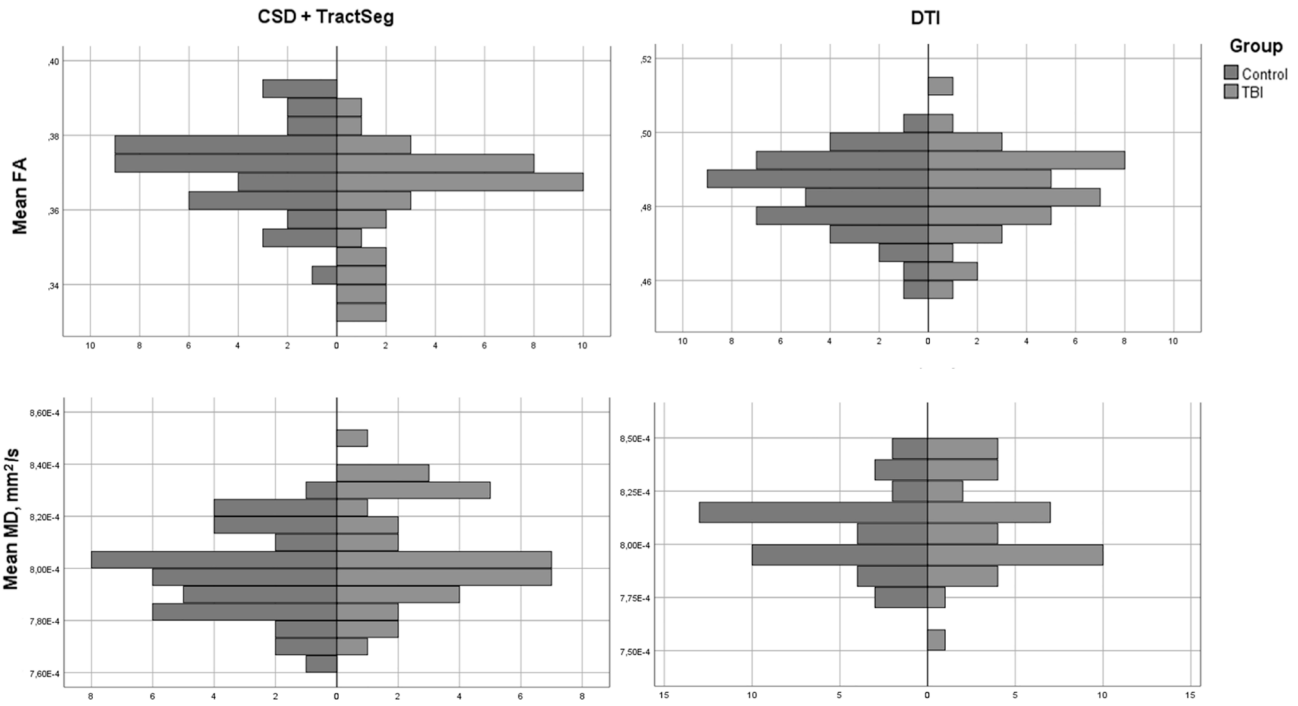

Fig. 3. Pyramid plots of the distribution of mean MD and mean FA. Upper row, FA values; lower row, MD values. Left column, CSD + TractSeg; right column, DTI. On X axis is frequency (n of participants). Left side of each pyramid plot represents the controls and right side TBI group.

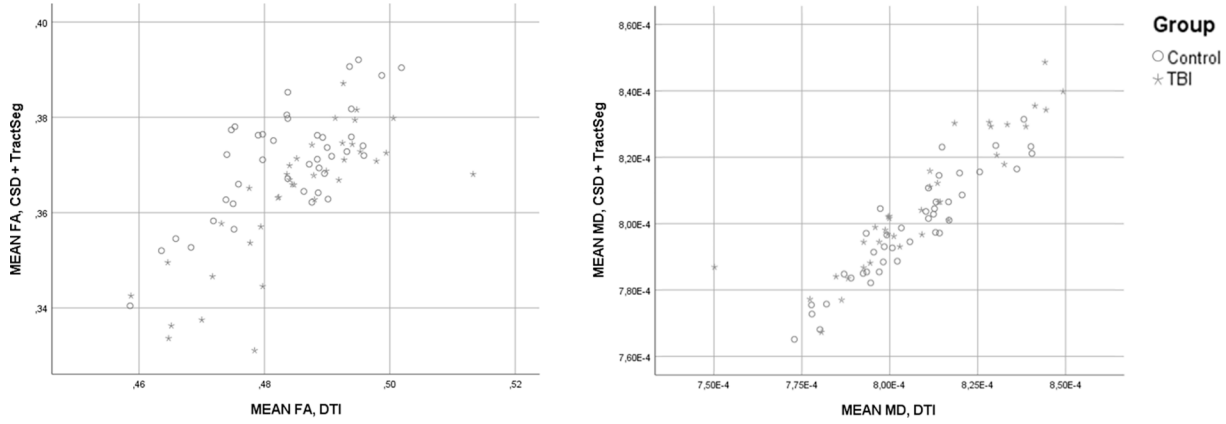

Fig. 4. Scatter plots of mean FA and MD values. X axis represents values derived from DTI tractography and Y axis values from CSD + TractSeg tractography. Control group participants are represented by green circles and TBI group participants by grey asterisks.

had lower FA, which is consistent with previous studies and has been interpreted as a sign of microstructural white matter injury (Borja et al., 2018; Eierud et al., 2014). There was also an interaction of tractography method and participant group on MD values in the main analysis (although in the alternative analysis with more limited preprocessing this effect was lost). Higher MD values of the TBI group compared to control group in CSD and TractSeg tractography possibly underlie this weaker interaction, but could not be conclusively demonstrated.

Using more advanced DWI processing methods such as CSD does not necessarily require newest high-end image acquisition but can be feasible with b = 800 s/mm^2 and 15 gradient directions data, if combined with appropriate tract reconstruction methods. However, a higher b-value and gradient number imaging is recommended, if available, as the ability to resolve crossing fibres with CSD is better with higher b-values (Tournier et al., 2008). Based on our results, TractSeg is a feasible method for reconstructing TBI patients' tracts. Once analysis pipeline is established, it is faster than reconstructing the same tracts based on manual ROI definitions and reduces the need for subjective judgement and neuroanatomical expertise. Our study thus demonstrates a potential method to increase the sensitivity and reliability of tract analysis and reduce workload.

The values acquired by DTI and CSD-based tractography methods were generally moderately to strongly correlated. The distributions of FA and MD values were similar and largely overlapping between the groups, but CSD specifically seemed to find relatively low FA values in more participants of the TBI group than DTI did. This suggests a subset of the TBI participants with more pronounced microstructural injuries, that were better identified by the CSD and TractSeg approach, although a causal link between these findings and the initial injury cannot be established by this study.

Correlations were not found between GCS, GOSE, and PTA and the tractography results. There are mixed reports of tractography statistics correlating (Kraus et al., 2007; Kumar et al., 2009; Lipton et al., 2009; Mohammadian et al., 2020, 2017; Niogi et al., 2008) or not correlating

(Churchill et al., 2017; Studerus-Germann et al., 2018; Wäljas et al., 2015; Wäljas et al., 2014) with clinical variables. Although by far not a unique feature of our study, the lack of correlation might be considered to cast doubt on the clinical validity of the results. However, several explanations for this shortcoming may be considered, namely the challenges related to TBI severity stratification and outcome evaluation, the multifactorial aetiology of long-term symptoms, and methodological issues generally related to tractography studies.

In our sample all TBI participants had an injury initially diagnosed as mild TBI based on the initial GCS and majority had a GCS score of 15. Therefore, GCS variability was low and might explain lack of correlation to tractography results. With regards to GOSE, all patients in the TBI sample showed incomplete recovery (GOSE < 8). Thus, patients with complete recovery were not in the analysis, and this might hamper finding correlations with tractography in the patient group. While GOSE is widely used and validated as a tool for measuring functional outcome, it has also been criticised for lacking inter-rater reliability and sensitivity especially in grading long-term symptoms related to mild TBI (McMillan et al., 2016). Addition of separate measures of cognitive outcome to TBI studies has been advocated (Bagiella et al., 2010) and could be especially helpful in studies of mild TBI.

Post-TBI symptoms are thought to represent the outcome of complex biopsychosocial interactions, where also other factors besides white matter injury may have important contributions. These may include e.g., post-traumatic stress disorder, prior physical and mental health, involvement in litigation, extra-cranial injuries, pain, and emotional distress (Carroll et al., 2004; Iverson, 2006; Iverson and Lange, 2003; Iverson and McCracken, 2009; Van Der Naalt et al., 2017; Wäljas et al., 2015). Therefore, although we expected microstructural white matter injury to contribute to long-term symptoms, correlation to symptoms may be obscured by other factors.

On the other hand, we may still be unable to detect some significant injuries with the present techniques, and thus unable to account for some injury-related symptoms by imaging. Improvements in imaging technique may help, but inherent problems are also caused by the sizeable inter-individual variation in tractography statistics. TBI-associated tractography findings are not disease-specific, and similar changes have been reported in e.g. psychiatric conditions, substance use, and sleep deprivation, with baseline cognitive capacity also potentially modifying the results (Dizaji et al., 2021; Elvsåshagen et al., 2015; Hampton et al., 2019; Jiang et al., 2017; Lipton et al., 2012).

Additionally, we found that FA and MD values calculated from DTI and CSD + TractSeg-based tractography were generally different. CSD + TractSeg resulted in lower FA and MD than DTI. Also, the relative values of different tracts were different, with e.g., the corpus callosum having the highest FA in the DTI analysis, but superior longitudinal fasciculi having the highest FA in CSD + TractSeg. On a general level, these findings reflect the methodological differences between the tractography methods. Tracts reconstructed by such different methods are not expected to be directly comparable, as there are fundamental differences in how they are defined (Schilling et al., 2021). As demonstrated in Fig. 1, CSD and TractSeg resulted in tracts with higher volume and extension closer to the cortical interface. This can explain why average FA was lower in CSD-based analysis. In deterministic DTI tractography the fibers will be terminated if FA falls below the predefined limit. A sufficiently strict FA limit is required to prevent tracking of fibres that are not anatomically related to the target tract. In TractSeg, lower FA volumes that are still actually related to the target tract may be included in the tract, as tracts are directly segmented from the fODF, utilising a pretrained convolutional neural network. Based on the present results and also the study by Ressel et al., 2018 (Ressel et al., 2018), such lower FA areas may however be highly clinically significant.

Seemingly small changes in tractography parameters can also result in substantial differences in the results, as exemplified here by the relatively high FA of corpus callosum in DTI tractography. This is related to the fact that we chose a tract termination minimum FA limit of 0.5 for the corpus callosum (to avoid excessive propagation of the tract), but 0.3 for other tracts. These findings do not pose a problem for our analysis, as the TBI and control group were analysed identically, but serve to highlight some of the potential challenges in generating normative data for clinical tractography (cf. Jones et al., 2013). Different relative FA and MD values may also be a reflection of how the tractography methods handle crossing fibres. The corpus callosum has highly parallel fibres, while association tracts have more crossing fibres, which results in lower DTI-based FA values. Crossing fibres should be better addressed by CSD, possibly explaining the relatively high FA derived from e.g. the superior longitudinal fasciculi with CSD + TractSeg.

Besides different diffusion model and tractography method, different preprocessing steps in the CSD and DTI based analysis pipelines might have influenced our results (Maximov et al., 2019; Oldham et al., 2020). In this study, DTI preprocessing utilised an older, commercial preprocessing tool compatible with the tractography software, while preprocessing pipeline for CSD data was more modern, including denoising and Gibbs and bias field corrections. To control for possible effects, we did an alternative CSD and TractSeg based analysis, utilising preprocessing similar to what was done in DTI pipeline. This gave mostly equivalent results (including our main finding of CSD + TractSeg being able to differentiate the groups based on FA, while DTI was not). As problems in signal-to-noise-ratio are more prevalent in higher b-value imaging (Maximov et al., 2019), it may be that our results are not particularly strongly affected by preprocessing approaches such as denoising. Still, some differences were also observed, highlighting the importance of considering preprocessing approaches in diffusion MRI studies.

Limitations of this study include the relatively low b-value and gradient number DWI acquisition, which limits tractography quality. However, an important outcome was that it is nevertheless possible to perform CSD-based tractography and obtain an apparent advantage in terms of sensitivity. The compared tractography approaches were different in several aspects, which makes it impossible to pinpoint a single reason why their performance was different. It must also be noted that patients with mass lesions were excluded, so applicability in such circumstances is not ascertained. GOSE was used as the outcome measure, but quantitative cognitive test results would have been a valuable addition. Estimates of premorbid cognitive functioning might also have been a valuable covariate in the analyses. Our TBI sample was heterogeneous in terms of time from injury to imaging, although this was not found to influence the results. The sample cannot be considered representative of mild TBI in general, as we used a selected sample with persistent TBI-related symptoms and GOSE < 8. Finally, we used healthy controls, which has been customary in many comparable studies. It can be argued that general trauma patients without TBI would make a better control group (Carroll et al., 2004), as they would better control for risk factors associated with being injured in the first place and non-specific injury related effects (such as pain and emotional distress). Comparing to TBI patients with good recovery would also have allowed more convincing hypotheses to be drawn about the clinical significance of the FA alterations we found.

5. Conclusion

Tractography based on CSD and automatic segmentation with TractSeg was able to discriminate a group of patients with TBI from healthy controls, while DTI-based tractography was not. CSD and TractSeg demonstrated lower FA values in the TBI group than in the control group. In combination with TractSeg it is feasible to use CSD with a lower b-value and a smaller number of gradient directions DWI data than previously reported.

Declaration of Competing Interest

The authors declare that they have no known competing financial

interests or personal relationships that could have appeared to influence the work reported in this paper.

Data availability

Data will be made available on request.

Funding

JT received funding from the University of Turku Graduate School.

JPP is funded by the Academy of Finland (grant 17379) and the Maire Taponen foundation.

TR received funding from the Finnish Cultural Foundation.

References

Ades-Aron, B., Veraart, J., Kochunov, P., McGuire, S., Sherman, P., Kellner, E., Novikov, D.S., Fieremans, E., 2018. Evaluation of the accuracy and precision of the diffusion parameter EStImation with Gibbs and NoisE removal pipeline. Neuroimage 183, 532–543. https://doi.org/10.1016/J.NEUROIMAGE.2018.07.066.

Alexander, A.L., Lee, J.E., Lazar, M., Field, A.S., 2007. Diffusion Tensor Imaging of the Brain. Neurotherapeutics 4, 316–329. https://doi.org/10.1016/j.nurt.2007.05.011.

Andersson, J.L.R., Sotiropoulos, S.N., 2016. An integrated approach to correction for off-resonance effects and subject movement in diffusion MR imaging. Neuroimage 125, 1063–1078. https://doi.org/10.1016/J.NEUROIMAGE.2015.10.019.

Andreasen, S.H., Andersen, K.W., Conde, V., Dyrby, T.B., Puonti, O., Kammersgaard, L. P., Madsen, C.G., Madsen, K.H., Poulsen, I., Siebner, H.R., 2020. Limited Colocalization of Microbleeds and Microstructural Changes after Severe Traumatic Brain Injury. J. Neurotrauma 37, 581–592. https://doi.org/10.1089/NEU.2019.6608/FORMAT/EPUB.

Auriat, A.M., Borich, M.R., Snow, N.J., Wadden, K.P., Boyd, L.A., 2015. Comparing a diffusion tensor and non-tensor approach to white matter fiber tractography in chronic stroke. NeuroImage Clin. 7, 771–781. https://doi.org/10.1016/j.nicl.2015.03.007.

Bagiella, E., Novack, T.A., Ansel, B., Diaz-Arrastia, R., Dikmen, S., Hart, T., Temkin, N., 2010. Measuring outcome in traumatic brain injury treatment trials: Recommendations from the traumatic brain injury clinical trials network. J. Head Trauma Rehabil. 25, 375–382. https://doi.org/10.1097/HTR.0b013e3181d27fe3.

Basser, P.J., Pajevic, S., Pierpaoli, C., Duda, J., Aldroubi, A., 2000. In vivo fiber tractography using DT-MRI data. Magn. Reson. Med. 44, 625–632. https://doi.org/10.1002/1522-2594(200010)44:4<625::AID-MRM17>3.0.CO;2-O.

Basser, P.J., Pierpaoli, C., 1996. Microstructural and physiological features of tissues elucidated by quantitative-diffusion-tensor MRI. J. Magn. Reson. B 111, 209–219. https://doi.org/10.1006/JMRB.1996.0086.

Bazarian, J.J., Zhong, J., Blyth, B., Zhu, T., Kavcic, V., Peterson, D., 2007. Diffusion Tensor Imaging Detects Clinically Important Axonal Damage after Mild Traumatic Brain Injury: A Pilot Study. J. Neurotrauma 24, 1447–1459. https://doi.org/10.1089/neu.2007.0241.

Becker, D., Scherer, M., Neher, P., Jungk, C., Jesser, J., Pflüger, I., Brinster, R., Bendszus, M., Bruckner, T., Maier-Hein, K., Unterberg, A., 2020. Going Beyond Diffusion Tensor Imaging Tractography in Eloquent Glioma Surgery–High-Resolution Fiber Tractography: Q-Ball or Constrained Spherical Deconvolution? World Neurosurg. 134, e596–e609. https://doi.org/10.1016/j.wneu.2019.10.138.

Borja, M.J., Chung, S., Lui, Y.W., 2018. Diffusion MR Imaging in Mild Traumatic Brain Injury. Neuroimaging Clin. N. Am. 28 (1), 117–126.

Brandstack, N., Kurki, T., Tenovuo, O., 2013. Quantitative Diffusion-Tensor Tractography of long association Tracts in Patients with Traumatic Brain injury without associated Findings at routine Mr imaging 1. Radiology 267. https://doi.org/10.1148/radiol.12112570/-/DC1.

Bullock, D., Takemura, H., Caiafa, C.F., Kitchell, L., McPherson, B., Caron, B., Pestilli, F., 2019. Associative white matter connecting the dorsal and ventral posterior human cortex. Brain Struct. Funct. 224, 2631–2660. https://doi.org/10.1007/s00429-019-01907-8.

Calamuneri, A., Arrigo, A., Mormina, E., Milardi, D., Cacciola, A., Chillemi, G., Marino, S., Gaeta, M., Quartarone, A., 2018. White matter tissue quantification at Low b-values within constrained spherical deconvolution framework. Front. Neurol. 9, 1–14. https://doi.org/10.3389/fneur.2018.00716.

Carroll, L., Cassidy, J.D., Peloso, P., Borg, J., von Holst, H., Holm, L., Paniak, C., Pépin, M., 2004. Prognosis for mild traumatic brain injury: Results of the WHO Collaborating Centre Task Force on Mild Traumatic Brain Injury. J. Rehabil. Med. Suppl. 36 (0), 84–105.

Churchill, N.W., Hutchison, M.G., Richards, D., Leung, G., Graham, S.J., Schweizer, T.A., 2017. Neuroimaging of sport concussion: persistent alterations in brain structure and function at medical clearance. Sci. Rep. 7 https://doi.org/10.1038/S41598-017-07742-3.

Cubon, V.A., Murugavel, M., Holmes, K.W., Dettwiler, A., 2018. Preliminary evidence from a prospective DTI study suggests a posterior-to-anterior pattern of recovery in college athletes with sports-related concussion. Brain Behav. 8 https://doi.org/10.1002/BRB3.1165/FORMAT/PDF.

Dinkel, J., Drier, A., Khalilzadeh, O., Perlbarg, V., Czernecki, V., Gupta, R., Gomas, F., Sanchez, P., Dormont, D., Galanaud, D., Stevens, R.D., Puybasset, L., 2014. Long-term white matter changes after severe traumatic brain injury: A 5-year prospective cohort. Am. J. Neuroradiol. 35 (1), 23–29.

Dizaji, A.S., Vieira, B.H., Khodaei, M.R., Ashrafi, M., Parham, E., Hosseinzadeh, G.A., Salmon, C.E.G., Soltanianzadeh, H., 2021. Linking brain biology to intellectual endowment: A review on the associations of human intelligence with neuroimaging data. Basic Clin. Neurosci. https://doi.org/10.32598/bcn.12.1.574.1.

Eierud, C., Craddock, R.C., Fletcher, S., Aulakh, M., King-Casas, B., Kuehl, D., Laconte, S. M., 2014. Neuroimaging after mild traumatic brain injury: Review and meta-analysis. NeuroImage Clin. 4, 283–294. https://doi.org/10.1016/j.nicl.2013.12.009.

Elvsåshagen, T., Norbom, L.B., Pedersen, P.Ø., Quraishi, S.H., Bjørnerud, A., Malt, U.F., Groote, I.R., Westlye, L.T., Najbauer, J., 2015. Widespread Changes in White Matter Microstructure after a Day of Waking and Sleep Deprivation. PLoS One 10 (5), e0127351.

Haber, M., Amyot, F., Lynch, C.E., Sandsmark, D.K., Kenney, K., Werner, J.K., Moore, C., Flesher, K., Woodson, S., Silverman, E., Chou, Y., Pham, D., Diaz-Arrastia, R., 2021. Imaging biomarkers of vascular and axonal injury are spatially distinct in chronic traumatic brain injury. J. Cereb. Blood Flow Metab. 41, 1924–1938. https://doi.org/10.1177/0271678X20985156.

Håberg, A.K., Olsen, A., Moen, K.G., Schirmer-Mikalsen, K., Visser, E., Finnanger, T.G., Evensen, K.A.I., Skandsen, T., Vik, A., Eikenes, L., 2015. White matter microstructure in chronic moderate-to-severe traumatic brain injury: Impact of acute-phase injury-related variables and associations with outcome measures. J. Neurosci. Res. 93, 1109–1126. https://doi.org/10.1002/JNR.23534.

Hampton, W.H., Hanik, I.M., Olson, I.R., 2019. Substance abuse and white matter: Findings, limitations, and future of diffusion tensor imaging research. Drug Alcohol Depend 197, 288–298.

Hulkower, M.B., Poliak, D.B., Rosenbaum, S.B., Zimmerman, M.E., Lipton, M.L., 2013. A Decade of DTI in Traumatic Brain Injury: 10 Years and 100 Articles Later. Am. J. Neuroradiol. 34, 2064–2074. https://doi.org/10.3174/AJNR.A3395.

Hunter, L.E., Lubin, N., Glassman, N.R., Xue, X., Spira, M., Lipton, M.L., 2019. Comparing Region of Interest versus Voxel-Wise Diffusion Tensor Imaging Analytic Methods in Mild and Moderate Traumatic Brain Injury: A Systematic Review and Meta-Analysis. J. Neurotrauma 36, 1222–1230. https://doi.org/10.1089/neu.2018.5838.

Iverson, G.L., 2006. Misdiagnosis of the persistent postconcussion syndrome in patients with depression. Arch. Clin. Neuropsychol. 21, 303–310. https://doi.org/10.1016/J.ACN.2005.12.008.

Iverson, G.L., McCracken, L.M., 2009. 'Postconcussive' symptoms in persons with chronic pain. https://doi.org.ezproxy.utu.fi/10.1080/026990597122990 11, 783–790. https://doi.org/10.1080/026990597122990.

Iverson, G.L., Lange, R.T., 2003. Examination of "postconcussion-like" symptoms in a healthy sample. Appl. Neuropsychol. 10, 137–144. https://doi.org/10.1207/S15324826AN1003_02.

Jeurissen, B., Leemans, A., Jones, D.K., Tournier, J.D., Sijbers, J., 2011. Probabilistic fiber tracking using the residual bootstrap with constrained spherical deconvolution. Hum. Brain Mapp. 32, 461–479. https://doi.org/10.1002/HBM.21032/FORMAT/PDF.

Jeurissen, B., Leemans, A., Tournier, J.D., Jones, D.K., Sijbers, J., 2013. Investigating the prevalence of complex fiber configurations in white matter tissue with diffusion magnetic resonance imaging. Hum. Brain Mapp. 34, 2747–2766. https://doi.org/10.1002/HBM.22099.

Jeurissen, B., Tournier, J.-D., Dhollander, T., Connelly, A., Sijbers, J., 2014. Multi-tissue constrained spherical deconvolution for improved analysis of multi-shell diffusion MRI data. Multi-tissue constrained spherical deconvolution for improved analysis of multi-shell diffusion MRI data. 103, 411–426.

Jiang, J., Zhao, Y.-J., Hu, X.-Y., Du, M.-Y., Chen, Z.-Q., Wu, M., Li, K.-M., Zhu, H.-Y., Kumar, P., Gong, Q.-Y., 2017. Microstructural brain abnormalities in medication-free patients with major depressive disorder: a systematic review and meta-analysis of diffusion tensor imaging. J Psychiatry Neurosci 42 (3), 150–163.

Jones, D.K., Knösche, T.R., Turner, R., 2013. White matter integrity, fiber count, and other fallacies: The do's and don'ts of diffusion MRI. Neuroimage 73, 239–254.

Kellner, E., Dhital, B., Kiselev, V.G., Reisert, M., 2016. Gibbs-ringing artifact removal based on local subvoxel-shifts. Magn. Reson. Med. 76, 1574–1581. https://doi.org/10.1002/MRM.26054.

Kraus, M.F., Susmaras, T., Caughlin, B.P., Walker, C.J., Sweeney, J.A., Little, D.M., 2007. White matter integrity and cognition in chronic traumatic brain injury: a diffusion tensor imaging study. Brain 130, 2508–2519. https://doi.org/10.1093/brain/awm216.

Kruper, J., Yeatman, J.D., Richie-Halford, A., Bloom, D., Grotheer, M., Caffarra, S., Kiar, G., Karipidis, I.I., Roy, E., Chandio, B.Q., Garyfallidis, E., Rokem, A., 2021. Evaluating the Reliability of Human Brain White Matter Tractometry. Aperture Neuro 2021, 2021–2022. https://doi.org/10.52294/e6198273-b8e3-4b63-babb-6e6b0da10669.

Kumar, R., Gupta, R.K., Husain, M., Chaudhry, C., Srivastava, A., Saksena, S., Rathore, R. K.S., 2009. Comparative evaluation of corpus callosum DTI metrics in acute mild and moderate traumatic brain injury: Its correlation with neuropsychometric test. Brain Inj. 23, 675–685. https://doi.org/10.1080/02699050903014915.

Lin, M., He, H., Schifitto, G., Zhong, J., 2016. Simulation of changes in diffusion related to different pathologies at cellular level after traumatic brain injury. Magn. Reson. Med. 76, 290–300. https://doi.org/10.1002/MRM.25816/FORMAT/PDF.

Lipton, M.L., Gulko, E., Zimmerman, M.E., Friedman, B.W., Kim, M., Gellella, E., Gold, T., Shifteh, K., Ardekani, B.A., Branch, C.A., 2009. Diffusion-tensor imaging implicates prefrontal axonal injury in executive function impairment following very mild traumatic brain injury. Radiology 252, 816–824. https://doi.org/10.1148/radiol.2523081584.

Lipton, M.L., Kim, N., Park, Y.K., Hulkower, M.B., Gardin, T.M., Shifteh, K., Kim, M., Zimmerman, M.E., Lipton, R.B., Branch, C.A., 2012. Robust detection of traumatic axonal injury in individual mild traumatic brain injury patients: intersubject variation, change over time and bidirectional changes in anisotropy. Brain Imaging Behav. 6, 329–342. https://doi.org/10.1007/S11682-012-9175-2.

Maier-Hein, K.H., Neher, P.F., Houde, J.-C., Côté, M.-A., Garyfallidis, E., Zhong, J., Chamberland, M., Yeh, F.-C., Lin, Y.-C., Ji, Q., Reddick, W.E., Glass, J.O., Chen, D.Q., Feng, Y., Gao, C., Wu, Y.e., Ma, J., He, R., Li, Q., Westin, C.-F., Deslauriers-Gauthier, S., González, J.O.O., Paquette, M., St-Jean, S., Girard, G., Rheault, F., Sidhu, J., Tax, C.M.W., Guo, F., Mesri, H.Y., Dávid, S., Froeling, M., Heemskerk, A. M., Leemans, A., Boré, A., Pinsard, B., Bedetti, C., Desrosiers, M., Brambati, S., Doyon, J., Sarica, A., Vasta, R., Cerasa, A., Quattrone, A., Yeatman, J., Khan, A.R., Hodges, W., Alexander, S., Romascano, D., Barakovic, M., Auría, A., Esteban, O., Lemkaddem, A., Thiran, J.-P., Cetingul, H.E., Odry, B.L., Mailhe, B., Nadar, M.S., Pizzagalli, F., Prasad, G., Villalon-Reina, J.E., Galvis, J., Thompson, P.M., Requejo, F. D.S., Laguna, P.L., Lacerda, L.M., Barrett, R., Dell'Acqua, F., Catani, M., Petit, L., Caruyer, E., Daducci, A., Dyrby, T.B., Holland-Letz, T., Hilgetag, C.C., Stieltjes, B., Descoteaux, M., 2017. The challenge of mapping the human connectome based on diffusion tractography. Nat Commun 8 (1).

Maximov, I.I., Alnæs, D., Westlye, L.T., 2019. Towards an optimised processing pipeline for diffusion magnetic resonance imaging data: Effects of artefact corrections on diffusion metrics and their age associations in UK Biobank. Hum. Brain Mapp. 40, 4146–4162. https://doi.org/10.1002/HBM.24691.

Mayer, A.R., Ling, J., Mannell, M.V., Gasparovic, C., Phillips, J.P., Doezema, D., Reichard, R., Yeo, R.A., 2010. A prospective diffusion tensor imaging study in mild traumatic brain injury. Neurology 74 (8), 643–650.

McGinn, M.J., Povlishock, J.T., 2016. Pathophysiology of Traumatic Brain Injury. Neurosurg. Clin. N. Am. 27 (4), 397–407.

McMillan, T., Wilson, L., Ponsford, J., Levin, H., Teasdale, G., Bond, M., 2016. The Glasgow Outcome Scale — 40 years of application and refinement. Nat. Publ. Gr. 12 (8), 477–485.

Mohammadian, M., Roine, T., Hirvonen, J., Kurki, T., Ala-Seppälä, H., Frantzén, J., Katila, A., Kyllönen, A., Maanpää, H.R., Posti, J., Takala, R., Tallus, J., Tenovuo, O., 2017. High angular resolution diffusion-weighted imaging in mild traumatic brain injury. NeuroImage Clin. 13, 174–180. https://doi.org/10.1016/j.nicl.2016.11.016.

Mohammadian, M., Roine, T., Hirvonen, J., Kurki, T., Posti, J.P., Katila, A.J., Takala, R.S. K., Tallus, J., Maanpää, H.R., Frantzén, J., Hutchinson, P.J., Newcombe, V.F., Menon, D.K., Tenovuo, O., 2020. Alterations in Microstructure and Local Fiber Orientation of White Matter Are Associated with Outcome after Mild Traumatic Brain Injury. J. Neurotrauma 37, 2616–2623. https://doi.org/10.1089/NEU.2020.7081/FORMAT/EPUB.

Mormina, E., Arrigo, A., Calamuneri, A., Alafaci, C., Tomasello, F., Morabito, R., Marino, S., Longo, M., Vinci, S.L., Granata, F., 2016. Optic radiations evaluation in patients affected by high-grade gliomas: a side-by-side constrained spherical deconvolution and diffusion tensor imaging study. Neuroradiology 58, 1067–1075. https://doi.org/10.1007/s00234-016-1732-8.

Niogi, S.N., Mukherjee, P., Ghajar, J., Johnson, C., Kolster, R.A., Sarkar, R., Lee, H., Meeker, M., Zimmerman, R.D., Manley, G.T., McCandliss, B.D., 2008. Extent of microstructural white matter injury in postconcussive syndrome correlates with impaired cognitive reaction time: A 3T diffusion tensor imaging study of mild traumatic brain injury. American Journal of Neuroradiology. 29 (5), 967–973.

Oldham, S., Arnatkevičiūtė, A., Smith, R.E., Tiego, J., Bellgrove, M.A., Fornito, A., 2020. The efficacy of different preprocessing steps in reducing motion-related confounds in diffusion MRI connectomics. Neuroimage 222, 117252.

Reijmer, Y.D., Leemans, A., Heringa, S.M., Wielaard, I., Jeurissen, B., Koek, H.L., Biessels, G.J., Zhan, W., 2012. Improved Sensitivity to Cerebral White Matter Abnormalities in Alzheimer's Disease with Spherical Deconvolution Based Tractography. PLoS One 7 (8), e44074.

Ressel, V., van Hedel, H.J.A., Scheer, I., O'Gorman Tuura, R., 2018. Comparison of DTI analysis methods for clinical research: influence of pre-processing and tract selection methods. Eur. Radiol. Exp. 2 https://doi.org/10.1186/S41747-018-0066-1.

Rheault, F., De Benedictis, A., Daducci, A., Maffei, C., Tax, C.M.W., Romascano, D., Caverzasi, E., Morency, F.C., Corrivetti, F., Pestilli, F., Girard, G., Theaud, G., Zemmoura, I., Hau, J., Glavin, K., Jordan, K.M., Pomiecko, K., Chamberland, M., Barakovic, M., Goyette, N., Poulin, P., Chenot, Q., Panesar, S.S., Sarubbo, S., Petit, L., Descoteaux, M., 2020. Tractostorm: The what, why, and how of tractography dissection reproducibility. Hum Brain Mapp 41 (7), 1859–1874.

Rostowsky, K.A., Maher, A.S., Irimia, A., 2018. Macroscale White Matter Alterations Due to Traumatic Cerebral Microhemorrhages Are Revealed by Diffusion Tensor Imaging. Front. Neurol. 948. https://doi.org/10.3389/FNEUR.2018.00948.

Schilling, K.G., Rheault, F., Petit, L., Hansen, C.B., Nath, V., Yeh, F.C., Girard, G., Barakovic, M., Rafael-Patino, J., Yu, T., Fischi-Gomez, E., Pizzolato, M., Ocampo-Pineda, M., Schiavi, S., Canales-Rodríguez, E.J., Daducci, A., Granziera, C., Innocenti, G., Thiran, J.P., Mancini, L., Wastling, S., Cocozza, S., Petracca, M., Pontillo, G., Mancini, M., Vos, S.B., Vakharia, V.N., Duncan, J.S., Melero, H., Manzanedo, L., Sanz-Morales, E., Peña-Melián, Á., Calamante, F., Attyé, A., Cabeen, R.P., Korobova, L., Toga, A.W., Vijayakumari, A.A., Parker, D., Verma, R., Radwan, A., Sunaert, S., Emsell, L., De Luca, A., Leemans, A., Bajada, C.J., Haroon, H., Azadbakht, H., Chamberland, M., Genc, S., Tax, C.M.W., Yeh, P.H., Srikanchana, R., Mcknight, C.D., Yang, J.Y.M., Chen, J., Kelly, C.E., Yeh, C.H., Cochereau, J., Maller, J.J., Welton, T., Almairac, F., Seunarine, K.K., Clark, C.A., Zhang, F., Makris, N., Golby, A., Rathi, Y., O'Donnell, L.J., Xia, Y., Aydogan, D.B., Shi, Y., Fernandes, F.G., Raemaekers, M., Warrington, S., Michielse, S., Ramírez-Manzanares, A., Concha, L., Aranda, R., Meraz, M.R., Lerma-Usabiaga, G., Roitman, L., Fekonja, L.S., Calarco, N., Joseph, M., Nakua, H., Voineskos, A.N., Karan, P., Grenier, G., Legarreta, J.H., Adluru, N., Nair, V.A., Prabhakaran, V., Alexander, A.L., Kamagata, K., Saito, Y., Uchida, W., Andica, C., Abe, M., Bayrak, R. G., Wheeler-Kingshott, C.A.M.G., D'Angelo, E., Palesi, F., Savini, G., Rolandi, N., Guevara, P., Houenou, J., López-López, N., Mangin, J.F., Poupon, C., Román, C., Vázquez, A., Maffei, C., Arantes, M., Andrade, J.P., Silva, S.M., Calhoun, V.D., Caverzasi, E., Sacco, S., Lauricella, M., Pestilli, F., Bullock, D., Zhan, Y., Brignoni-Perez, E., Lebel, C., Reynolds, J.E., Nestrasil, I., Labounek, R., Lenglet, C., Paulson, A., Aulicka, S., Heilbronner, S.R., Heuer, K., Chandio, B.Q., Guaje, J., Tang, W., Garyfallidis, E., Raja, R., Anderson, A.W., Landman, B.A., Descoteaux, M., 2021. Tractography dissection variability: What happens when 42 groups dissect 14 white matter bundles on the same dataset? Neuroimage 243, 118502. https://doi.org/10.1016/J.NEUROIMAGE.2021.118502.

Shahim, P., Politis, A., van der Merwe, A., Moore, B., Ekanayake, V., Lippa, S.M., Chou, Y.Y., Pham, D.L., Butman, J.A., Diaz-Arrastia, R., Zetterberg, H., Blennow, K., Gill, J.M., Brody, D.L., Chan, L., 2020. Time course and diagnostic utility of NfL, tau, GFAP, and UCH-L1 in subacute and chronic TBI. e636 Neurology 95, e623. https://doi.org/10.1212/WNL.0000000000009985.

Studerus-Germann, A.M., Gautschi, O.P., Bontempi, P., Thiran, J.P., Daducci, A., Romascano, D., von Ow, D., Hildebrandt, G., von Hessling, A., Engel, D.C., 2018. Central nervous system microbleeds in the acute phase are associated with structural integrity by DTI one year after mild traumatic brain injury: A longitudinal study. Neurol. Neurochir. Pol. 52, 710–719. https://doi.org/10.1016/J.PJNNS.2018.08.011.

Tournier, J.-D., Calamante, F., Connelly, A., 2007. Robust determination of the fibre orientation distribution in diffusion MRI: Non-negativity constrained super-resolved spherical deconvolution. Robust determination of the fibre orientation distribution in diffusion MRI: Non-negativity constrained super-resolved spherical deconvolution. 35 (4), 1459–1472.

Tournier, J.D., Calamante, F., Connelly, A., 2013. Determination of the appropriate b value and number of gradient directions for high-angular-resolution diffusion-weighted imaging. NMR Biomed. 26, 1775–1786. https://doi.org/10.1002/nbm.3017.

Tournier, J.-D., Smith, R., Raffelt, D., Tabbara, R., Dhollander, T., Pietsch, M., Christiaens, D., Jeurissen, B., Yeh, C.-H., Connelly, A., 2019. MRtrix3: A fast, flexible and open software framework for medical image processing and visualisation. NeuroImage 202, 116137.

Tournier, J.D., Yeh, C.H., Calamante, F., Cho, K.H., Connelly, A., Lin, C.P., 2008. Resolving crossing fibres using constrained spherical deconvolution: Validation using diffusion-weighted imaging phantom data. Neuroimage 42, 617–625. https://doi.org/10.1016/j.neuroimage.2008.05.002.

Tuch, D.S., Reese, T.G., Wiegell, M.R., Makris, N., Belliveau, J.W., Wedeen, V.J., 2002. High angular resolution diffusion imaging reveals intravoxel white matter fiber heterogeneity. Magn. Reson. Med. 48, 577–582. https://doi.org/10.1002/MRM.10268.

Tustison, N.J., Avants, B.B., Cook, P.A., Zheng, Y., Egan, A., Yushkevich, P.A., Gee, J.C., 2010. N4ITK: Improved N3 bias correction. IEEE Trans. Med. Imaging 29, 1310–1320. https://doi.org/10.1109/TMI.2010.2046908.

Useche, J.N., Bermudez, S., 2018. Conventional Computed Tomography and Magnetic Resonance in Brain Concussion. Neuroimaging Clin. N. Am. 28 (1), 15–29.

van der Naalt, J., Timmerman, M.E., de Koning, M.E., van der Horn, H.J., Scheenen, M. E., Jacobs, B., Hageman, G., Yilmaz, T., Roks, G., Spikman, J.M., 2017. Early predictors of outcome after mild traumatic brain injury (UPFRONT): an observational cohort study. Artic. Lancet Neurol 16 (7), 532–540.

Veraart, J., Novikov, D.S., Christiaens, D., Ades-aron, B., Sijbers, J., Fieremans, E., 2016. Denoising of diffusion MRI using random matrix theory. Neuroimage 142, 394–406. https://doi.org/10.1016/j.neuroimage.2016.08.016.

Wäljas, M., Lange, R.T., Hakulinen, U., Huhtala, H., Dastidar, P., Hartikainen, K., Öhman, J., Iverson, G.L., 2014. Biopsychosocial outcome after uncomplicated mild traumatic brain injury. J. Neurotrauma 31, 108–124. https://doi.org/10.1089/NEU.2013.2941.

Wäljas, M., Iverson, G.L., Lange, R.T., Hakulinen, U., Dastidar, P., Huhtala, H., Liimatainen, S., Hartikainen, K., Öhman, J., 2015. A prospective biopsychosocial study of the persistent post-concussion symptoms following mild traumatic brain injury. J. Neurotrauma 32, 534–547. https://doi.org/10.1089/NEU.2014.3339.

Wasserthal, J., Neher, P., Maier-Hein, K.H., 2018. TractSeg - Fast and accurate white matter tract segmentation. Neuroimage 183, 239–253. https://doi.org/10.1016/j.neuroimage.2018.07.070.

Wasserthal, J., Neher, P.F., Hirjak, D., Maier-Hein, K.H., 2019. Combined tract segmentation and orientation mapping for bundle-specific tractography. Med. Image Anal. 58, 101559.

Wilde, E.A., McCauley, S.R., Hunter, J.V., Bigler, E.D., Chu, Z., Wang, Z.J., Hanten, G.R., Troyanskaya, M., Yallampalli, R., Li, X., Chia, J., Levin, H.S., 2008. Diffusion tensor imaging of acute mild traumatic brain injury in adolescents. Neurology 70, 948–955. https://doi.org/10.1212/01.wnl.0000305961.68029.54.

Yeatman, J.D., Dougherty, R.F., Myall, N.J., Wandell, B.A., Feldman, H.M., Beaulieu, C., 2012. Tract Profiles of White Matter Properties: Automating Fiber-Tract Quantification. PLoS One 7 (11), e49790.